International Journal of Heat and Mass Transfer 209 (2023) 124149

Contents lists available at ScienceDirect

International Journal of Heat and Mass Transfer

journal homepage: www.elsevier.com/locate/hmt

Multi-band and wide-angle nonreciprocal thermal radiation

Zihe Chen [a], Shilv Yu [a], Bin Hu [b], Run Hu [a,b,*]

[a] School of Energy and Power Engineering, Huazhong University of Science and Technology, Wuhan 430074, China
[b] Wuhan National Laboratory for Optoelectronics, Huazhong University of Science and Technology, Wuhan 430074, China

ARTICLE INFO

Article history:
Received 4 January 2023
Revised 14 March 2023
Accepted 26 March 2023

Keywords:
Kirchhoff's law
multi-band nonreciprocal thermal radiation
magneto-optical effect
cavity modes
aperiodic multilayer structure

ABSTRACT

Violating Kirchhoff's radiation law through magneto-optical materials or spatiotemporal (Floquet) metamaterials can open a new door for engineering thermal radiation by breaking the widely-accepted equal constraint of spectral absorptivity (α) and emissivity (ϵ). Most existing work only reports the unequal α and ϵ spectra in one or two bands and within limited angles. This significantly limits the practical applications like the nonreciprocal thermophotovoltaics. In this work, we present a general machine-learning-kernel-based algorithm framework, based on which we achieve four-band nonreciprocal thermal radiation via the magneto-optical (MO) materials. The realization of multi-band nonreciprocity is mainly attributed to the coupling effect of magneto-optical effect and the excitation of cavity modes with different orders, which can be confirmed by investigating the magnetic field distribution. In addition, it is found that dual-band/multi-band strong nonreciprocal thermal radiation can be realized in a wide range of incident angles (15°-85°). The number of bands and range of angle can be further enhanced by modulating the number of layers, structures, materials, and applied magnetic field. The present work offers a general design roadmap for nonreciprocal thermal radiation, and can be extended for designing metamaterials beyond thermal metamaterials.

1. Introduction

According to Kirchhoff's radiation law, for a given direction and frequency, the directional spectral emissivity (ϵ) should be equal to the directional spectral absorptivity (α), i.e. $\epsilon(\lambda,\theta)= \alpha(\lambda,\theta)$, which is valid for reciprocal thermal emitters [1–3] . Nevertheless, Kirchhoff's law is only a result of Lorentz reciprocity theorem rather than a requirement of thermodynamic law [4], which means that if the emitter contains nonreciprocal materials, Kirchhoff's law can be broken, i.e. $\epsilon(\lambda,\theta)\neq\alpha(\lambda,\theta)$. Therefore, the implementation of the nonreciprocal thermal emitter can provide the possibility for the separate control of emission and absorption, which can break the inherent energy loss mechanism in the photon recovery process to achieve higher energy recovery efficiency [5,6].

Since Zhu and Fan's pioneering work in 2014 [7], more and more nonreciprocal emitter structures have been proposed to violate Kirchhoff's radiation law by using the nonreciprocal materials, including magneto-optical materials [8–10] and Weyl semimetals [11–14]. For example, the nonreciprocal thermal emitter composed of a uniform metal layer and the n-InAs grating structure was proposed and almost achieved complete violation of Kirchhoff's law at wavelength of 16 μm with B = 3T at a large incident angle of 60° [7]. Wu et al. designed a one-dimensional (1D) magnetophotonic crystal structure and achieved the strong nonreciprocal thermal radiation at a incident angle of 30° [15]. In addition, recently, it has been found that the topological magnetic Weyl semimetals can realize the violation of Kirchhoff's law without the external magnetic field, mainly due to the anomalous Hall effect and the enhanced Berry curvature at Weyl nodes [13,16-18]. For instance, Chen et al. demonstrated that nonreciprocal surface plasmons can achieve obvious nonreciprocal thermal radiation without the external magnetic field by modeling and simulating the type-I Weyl semimetals [13]. Yu et al. showed that the excitation of the Tamm plasmon polaritons could also achieve the violation of Kirchhoff's law by constructing 1D photonic crystal structures containing Weyl semimetals [12]. Most existing researches mainly focus on the design of single-band nonreciprocal thermal emitters, while the practical devices may need multi-band and broadband nonreciprocal emission and absorption, such as filters, detectors, mid-infrared stealth and thermophotovoltaics devices [19,20]. Zhu et al. [21] proposed a gradient epsilon-near-zero magneto-optical metamaterial and achieved broadband nonreciprocal thermal emission. More recently, Qing et.al [22] proposed a nonreciprocal thermal emitter consisting of a topological photonic crystal embedded by a magnetic Weyl semimetal, which can realize the tri-channel nonreciprocal radiation. However, multi-band nonreciprocal thermal emitters composed of magneto-optical materials have been

* Corresponding author.
E-mail address: hurun@hust.edu.cn (R. Hu).

https://doi.org/10.1016/j.ijheatmasstransfer.2023.124149
0017-9310/

scarcely reported and there is still a lack of guidance for the design of multi-band nonreciprocal structures.

Currently, the structure design of nonreciprocal thermal emitters is mainly realized by grating guide mode structure [7,9] and 1D photonic crystal structure [23,24]. However, the fabrication of grating structure requires lithography technology, which is more complicated than that of 1D structure. In addition, the designs of 1D photonic crystals for nonreciprocal thermal radiation are usually periodic [15] or symmetrical structures [23]. The main reason is that the realization of nonreciprocal thermal radiation involves not only the design of the structure itself, but also the influence of other factors such as the external magnetic field, incident angle and so on, which makes the design more difficult. In addition, the design of aperiodic structures usually uses some special sequences, such as the Thue-morse sequence [24]. There are few researches on aperiodic structures with no regularity at all. That is to say, the structural design of nonreciprocal thermal radiation based on 1D multilayer structures still has a lot of optimization space.

In this work, we present a general machine-learning-kernel-based algorithm framework, based on which we can achieve single-band, dual-band and multi-band nonreciprocal thermal radiation via the coupling of the magneto-optical effect and the excitation of cavity modes. Based on this method, we propose a 32-layer aperiodic multilayer structure composed of InAs and SiO_2, which can achieve the strong violation of Kirchhoff's radiation law in four bands. In addition, by studying the influence of incident angle on the nonreciprocal thermal radiation, it is found that in a wide range of angles (15°-85°), the phenomenon of dual-band and multi-band nonreciprocal thermal radiation is common, which provides more options for the verification of nonreciprocal thermal radiation experiment.

2. Calculation methods

Here, we consider a 32-layer film structure composed of magneto-optical material InAs and the material SiO_2 to achieve the design of a multi-band nonreciprocal thermal emitter. As shown in Fig. 2 (b), there is an external magnetic field B along the y direction. At this time, the relative dielectric tensor of the material InAs is [24]

$$\varepsilon = \begin{bmatrix} \varepsilon_{xx} & 0 & \varepsilon_{xz} \\ 0 & \varepsilon_{yy} & 0 \\ \varepsilon_{zx} & 0 & \varepsilon_{zz} \end{bmatrix}, \tag{1}$$

where

$$\varepsilon_{xx} = \varepsilon_{zz} = \varepsilon_\infty - \frac{\omega_p^2(\omega + i\Gamma)}{\omega\left[(\omega + i\Gamma)^2 - \omega_c^2\right]}, \tag{2}$$

$$\varepsilon_{xz} = -\varepsilon_{zx} = i\frac{\omega_p^2\omega_c}{\omega\left[(\omega + i\Gamma)^2 - \omega_c^2\right]}, \tag{3}$$

$$\varepsilon_{yy} = \varepsilon_\infty - \frac{\omega_p^2}{\omega(\omega + i\Gamma)}, \tag{4}$$

In Eqs. (2)-(4), the specific definitions and parameter values are from Ref. [25]. In addition, to simplify the model, the refractive index of SiO_2 is 1.45 [23,24] and the metal Al is chosen as the bottom layer due to its high reflectivity. The permittivity of the Al is calculated according to the Drude model which is equal to the form of Eq. (4) and the parameters are found in Ref. [25].

Consider TM polarization plane wave in the x-z plane with an angle of incidence θ and only TM polarization is considered. The spectral directional absorptivity and emissivity can be obtained by calculating reflectivity and transmissivity and the specific formulas are [7]

$$\alpha(\theta, \lambda) = 1 - R(\theta, \lambda) - T(\theta, \lambda), \tag{5}$$

$$\epsilon(\theta, \lambda) = 1 - R(-\theta, \lambda) - T(-\theta, \lambda), \tag{6}$$

Here, $R(\theta, \lambda)$ and $R(-\theta, \lambda)$ are the spectral reflectivity for the angle θ and $-\theta$, respectively. $T(\theta, \lambda)$ and $T(-\theta, \lambda)$ are the spectral transmissivity for the angle θ and $-\theta$, respectively. The calculations of the reflectivity and transmissivity are achieved by the transfer matrix method (TMM) and the specific calculation details refer to Ref. [24,26].

However, for such binary sequences, there will be 2^{32} kinds of possible structures. In the face of such a large number of candidates, the traditional optimization methods appear to be inadequate. Here, we adopt the method of the Monte Carlo Tree Search (MCTS) algorithm combined with Bayesian optimization algorithm in the framework of python library MDTS (Material Design using Tree Search) to better achieve this goal [27–30] and the specific optimization process is shown in Fig. 1, including selection, expansion, simulation and back propagation. To meet the requirement of MCTS, we first digitize the two materials, i.e. digit 0 for InAs and digit 1 for SiO_2. Any sequence of the digits of 0 and 1 from the root node to the leaf node can correspond to the physical model of a multilayer film constructed by InAs and SiO_2. Then the corresponding absorptivity and emissivity spectra can be calculated by TMM and output the optimization target N which will be feedback to the MCTS algorithm for evaluating the performance of the corresponding sequence. Here, the optimization target N is the number of nonreciprocal bands, which meets the condition

$$N = \sum_{i=1}^{M} H(|\alpha_{Pi} - \epsilon_{Pi}| - \delta), \tag{7}$$

Here, $H(\ldots)$is the Heaviside function; $\alpha_{Pi}$is the absorptivity at the i-th peak of the absorption spectrum and ϵ_{Pi} is the emissivity at the corresponding wavelength; M is the number of peaks in the absorption spectrum; δ represents the degree of nonreciprocity (here $\delta = 0.8$). Therefore, by judging the difference between absorptivity and emissivity at the peak of the absorption spectrum, the above formula can obtain the number of nonreciprocal bands.

3. Results and discussions

Here, as shown in Fig. 2(a), the target value N represents the number of nonreciprocal bands. It can be seen that only 1121 iterations are calculated to find a four-band nonreciprocal emitter structure, which shows the high efficiency of this method in the design of multi-band nonreciprocal thermal emitters. The optimization result is a 32-layer structure and the corresponding sequence is 01110000001011100100100010101011, where the digit 1 represents the SiO_2 layer and the digit 0 represents the InAs layer. The corresponding physical model is shown in Fig. 2(b), with parameters B = 5T, d (the unit layer thickness of InAs) = 1.7 µm, d_1 (the unit layer thickness of SiO_2) = 3.1 µm, d_2 (the thickness of Al) = 0.2 µm and θ=60°. The calculated absorptivity and emissivity spectra for θ=60° with B = 0T and B = 5T are shown in Fig. 2 (c). When B = 0T, it can be seen that the absorptivity and emissivity spectra perfectly overlap, which means that there is no nonreciprocity. In addition, there are four sharp and narrow peaks and the values of the absorptivity (emissivity) can even reach about 1. With B = 5T, both absorption and emission peaks appear blue shift. Most importantly, the absorption and emissivity spectra no longer overlap, which indicates the violation of Kirchhoff's radiation law. Fig. 2(d) shows the difference between the absorptivity and emissivity and the difference at the wavelengths of 14.845 µm, 15.215 µm, 16.135 µm and 16.745 µm can reach 0.934, 0.959, 0.888 and 0.903, respectively. This phenomenon exhibits strong nonreciprocal

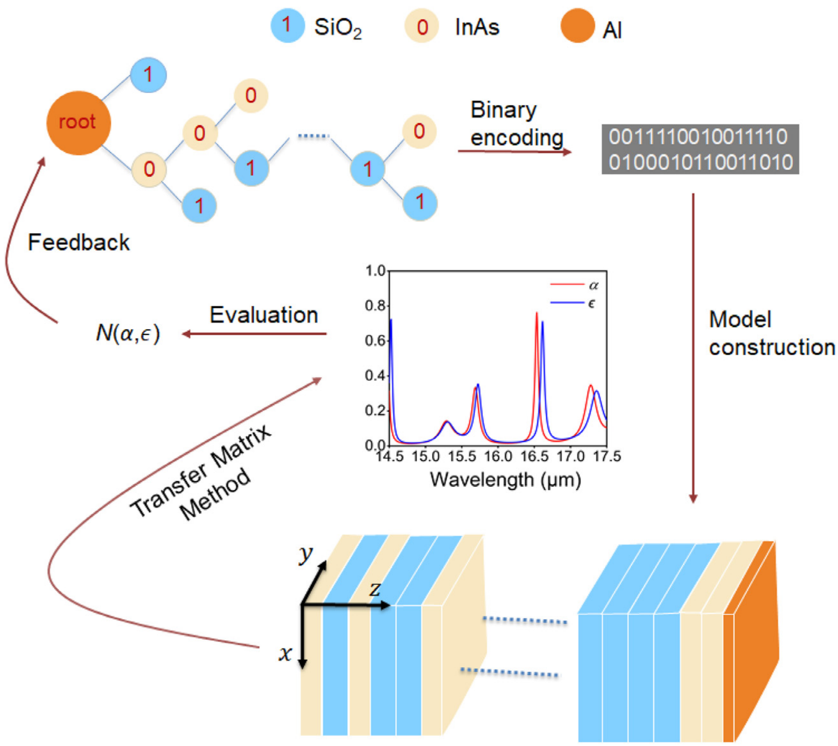

Fig. 1. Schematic diagram of multi-band nonreciprocal thermal radiation based on machine learning.

radiation and also demonstrates that our proposed structure has the property of multi-channel nonreciprocal thermal radiation.

In order to reveal the physical mechanism behind the nonreciprocal thermal radiation behavior, the magnetic field ($|H_y|$) distribution at the junction of metal Al and InAs is calculated and the result is shown in Fig. 3(a) and(b), where the red and blue lines represent the cases of θ= 60° and θ= -60°, respectively. When B = 0T, as shown in Fig. 3(a), in the wavelength range, there are four peaks of the magnetic field distribution, exactly corresponding to the absorption/emission spectrum with B=0T. In addition, the magnetic field distributions at the opposite angles almost overlap completely, which means there is no nonreciprocity. With B = 5T, it is clear that the magnetic field distributions at the opposite angles no longer coincide, mainly due to the magneto-optical effect. Also the peaks of the magnetic field distribution correspond to the resonant wavelengths in the absorption and emission spectra. Fig. 3(c) shows the magnetic field distribution along the z direction of the entire structure at wavelength of 14.845 μm. Besides, we also focus on showing the magnetic field around the bottom interface between the metal Al and the InAs film. Obviously, when θ= 60°, it is clear that the magnetic field amplitude is strongly enhanced at the bottom interface between the metallic mirror and the aperiodic magneto-optical crystal. In addition, the magnetic field amplitude tends to decrease as it moves away from the metal Al. This phenomenon occurs mainly because aperiodic multilayer structure can constitute classical microcavities and excite typical cavity modes [31], which makes the magnetic field realize local enhancement. Correspondingly, the enhanced magnetic field will increase the absorption of the structure, which can realize a high absorption at the wavelength of 14.845 μm. By contrast, with θ= -60°, there is barely enhancement of the magnetic field at the interface thus leading to the weak absorption. In order to better show the effect of cavity modes, we calculate the magnetic field distribution of multilayer structure without metal layer, as shown in Fig. 3(d). It can be seen that the magnetic field amplitude is relatively weak and the magnetic field distributions in the opposite directions basically coincide, which means that there is basically no nonreciprocal thermal radiation. This phenomenon proves that the realization of strong nonreciprocal thermal radiation is the result of the excitation of cavity modes at the interface between the bottom InAs and the metal Al [22].

Fig. 4 shows the angular distribution of the absorptance with B = 5T at four wavelengths, which correspond to the wavelengths with strong nonreciprocity. It can be seen that the absorptance at each wavelength is asymmetrical, which is mainly due to the magneto-optical effect caused by magneto-optical material InAs. In addition, at each wavelength, there are very sharp and strong absorption peaks only at certain angles, and the absorption at other angles is basically close to zero. In addition, the different intensity of absorption peaks at each wavelength can also be observed, which is mainly due to the different loss at the opposite angles caused by the asymmetric dielectric tensor of the magneto-optical material InAs.

The degree of the violation of Kirchhoff's radiation law depends on the intensity of the external magnetic field and the angle of incidence. Fig. 5 shows the difference $|\alpha$-$\epsilon|$ between absorptivity and emissivity as functions of angle of incidence and wavelength under different magnetic fields B. First of all, it can be seen from Fig. 5(a) that there are mainly four pairs of distinct separation bands with B = 5T, which represents the existence of four-band nonreciprocal thermal radiation. Secondly, with the decrease of incident angle, although the difference between absorptivity and emissivity is somewhat weakened, it can still obtain obvious multi-band/dual-band nonreciprocity in a wide range of angles, which provides more possibilities and options for the actual measurement of nonreciprocal thermal radiation. When B = 3T, as shown in Fig. 5(b), the absorptivity and emissivity peaks become less separated as the B field reduces, but it can also achieve a multi-band violation of Kirchhoff's radiation law. In addition, as the magnetic field decreases, it is clear to be seen that the nonreciprocal bands

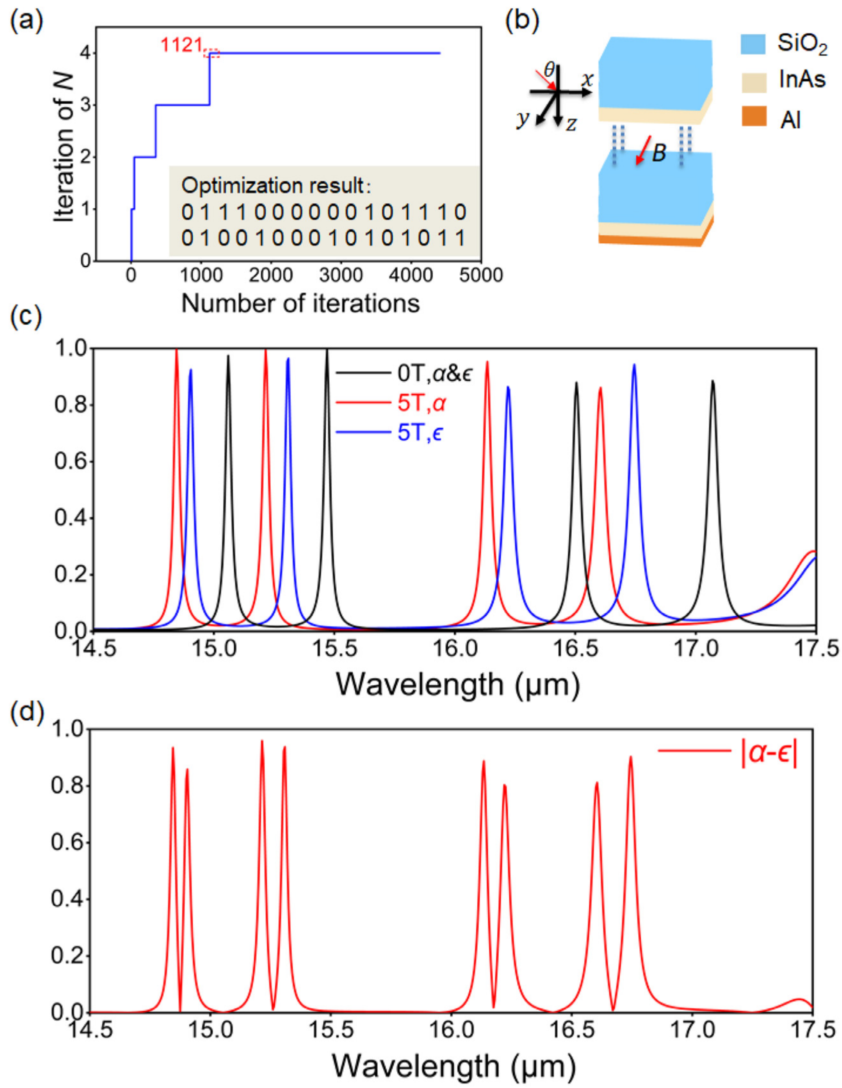

Fig. 2. (a) Tracing of the N iteration. (b) Physical model diagram corresponding to optimization results. (c) Absorptivity (α) and emissivity (ϵ) spectra at θ=60° for B = 0T and B = 5T. (d) Difference between the absorptivity and emissivity $|\alpha$-$\epsilon|$ with B = 5T.

are redshifted. Fig. 5(c) also shows the difference between the absorptivity and emissivity $|\alpha$-$\epsilon|$ at θ= 60° with B = 3T, which corresponds to the situation with the green dotted line in Fig. 5(b). As can be seen from Fig. 5(c), although the magnetic field is reduced to 3T, strong four-band nonreciprocal thermal radiation can still be achieved. The difference between the absorptivity and emissivity at the wavelengths of 14.975 μm, 15.425 μm, 16.36 μm and 16.97 μm can reach 0.853, 0.932, 0.793 and 0.845, respectively. Here, the mechanism of the above phenomenon is revealed by the variation of the dielectric tensor of the magneto-optical material InAs with the strength of magnetic field B and the wavelength, as shown in Fig. 5(d), where the red and green lines represent the cases of B = 5T and B = 3T, respectively. Since the strength of the magneto-optical effect is related to the value of $\varepsilon_{xz}/\varepsilon_{xx}$, the radio increases as the magnetic field B goes from 3T to 5T, which makes the absorptivity and emissivity peaks become more separated. Besides, the value of ε_{xx} decreases as the magnetic field increases, which makes the nonreciprocal bands blue shift when the magnetic field changes from 3T to 5T.

Fig. 6(a) and (b) respectively discuss the influence of thickness changes of InAs and SiO_2 on the degree of nonreciprocity of the whole structure at θ= 60° with B = 5T . As shown in Fig. 6(a), the thickness of SiO_2 layer remains unchanged, and the thickness of InAs layer is changed from 0.1 μm to 5 μm. It can be clearly seen that multiple pairs of separated bands, which represent multi-band nonreciprocal thermal radiation. However, it is obvious that multi-band nonreciprocal thermal radiation is greatly affected by the thickness of the magneto-optical material, which can be realized well within a small thickness range. Fig. 6(b) shows the effect of SiO_2 layer thickness on nonreciprocal thermal radiation and the multipair nonreciprocal band can also be seen. When the thickness of SiO_2 layer is within the blue dotted line range, the four-band nonreciprocal thermal radiation can be well realized and the thickness range is about 2.8 μm to 3.8 μm, which is a relatively wide thickness range. In addition, if the thickness of SiO_2 layer is in the range of the green dotted line, which is about 2.4 μm to 4.6 μm, the strong violation of Kirchhoff's radiation law can be well achieved in the dual/multi-band. Therefore, in our proposed structure, the properties of multi-band nonreciprocal thermal radiation are strongly influenced by the magneto-optical material InAs, while the thickness of SiO_2 layer can fluctuate over a wide range without affecting the nonreciprocal properties of the structure.

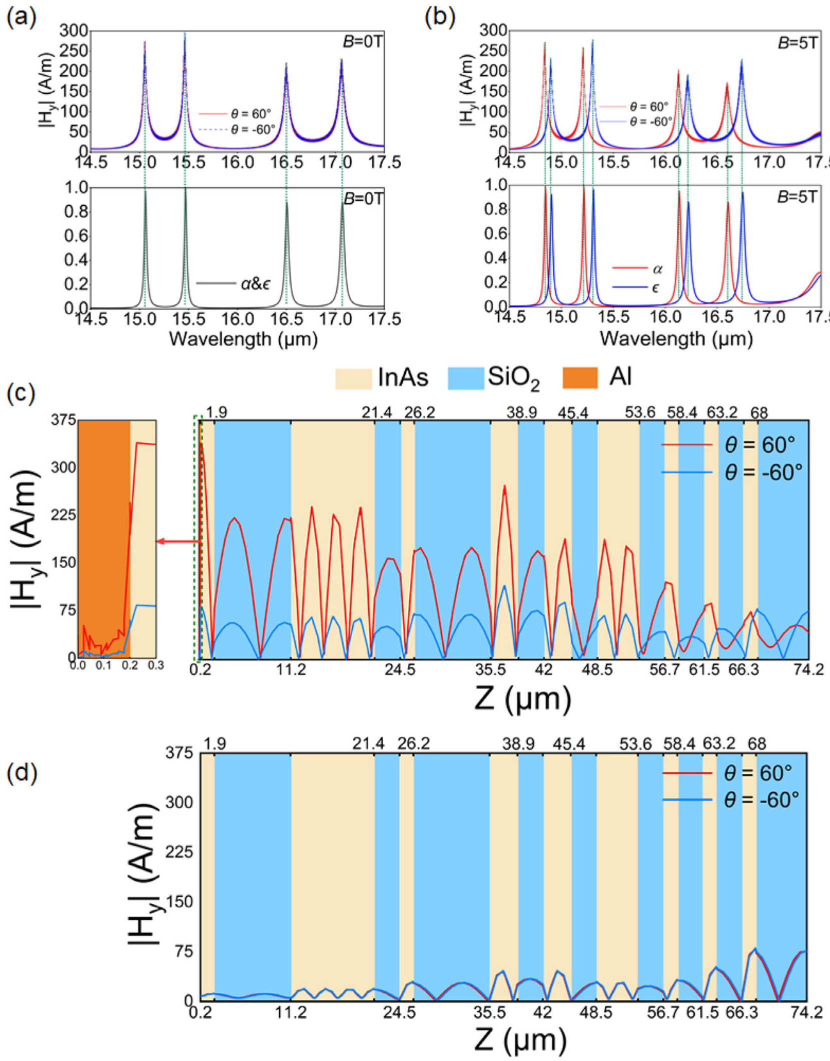

Fig. 3. (a) and (b) Magnetic field distribution $|H_y|$ at the junction of metal Al and InAs at θ= 60° and θ= -60° with B = 0T and B = 5T, respectively. The magnetic field distribution $|H_y|$ along z direction at the wavelength of 14.845 μm at θ= 60° and θ= -60° with B = 5T: (c) with metal layer; (d) without metal layer.

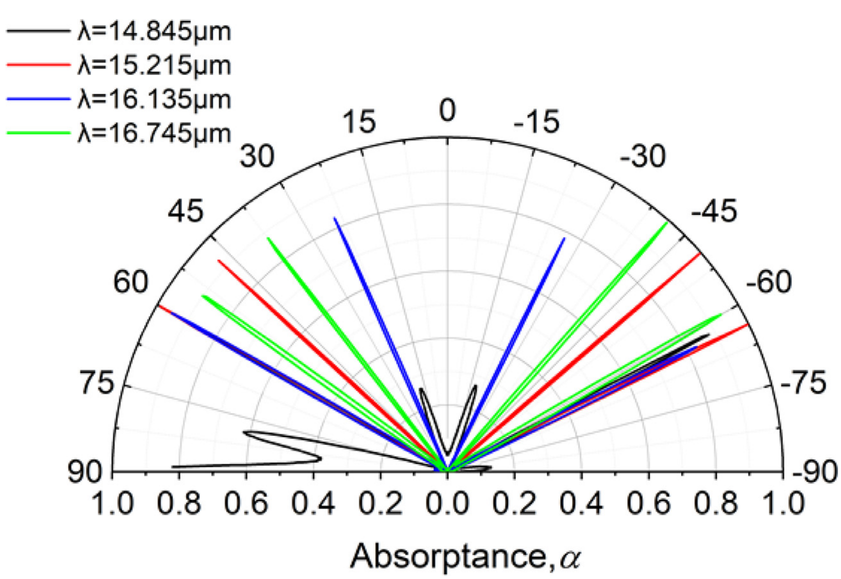

Fig. 4. Angular distribution diagram of absorptance at the specific wavelengths with B = 5T.

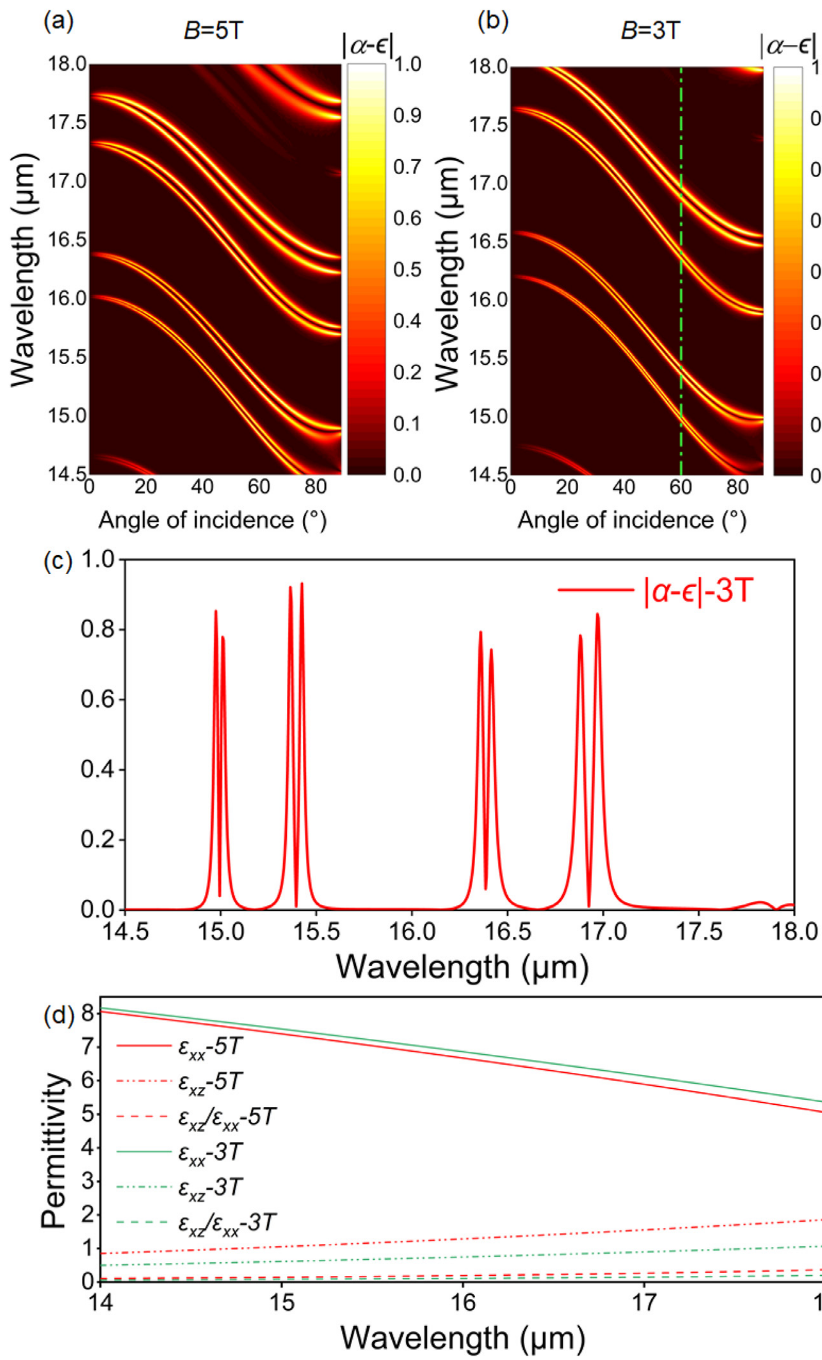

Fig. 5. (a, b) The difference between absorption and emission varies with incident angle and wavelength with B = 5T and B = 3T, respectively. (c) Difference between the absorptivity and emissivity $|\alpha\text{-}\epsilon|$ at θ= 60° with B = 3T. (d) The values of ε_{xx}, ε_{xz} and $\varepsilon_{xx}/\varepsilon_{xz}$ under different magnetic fields.

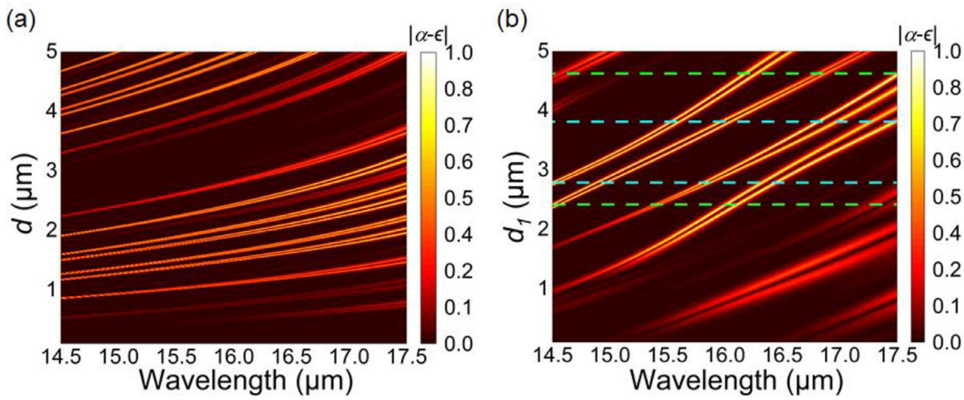

Fig. 6. (a) Difference between absorption and emission varies with the wavelength and the thickness of the InAs layer *d*. (b) Difference between absorption and emission varies with the wavelength and the thickness of the SiO_2 layer d_1.

4. Conclusion

In summary, we propose an aperiodic multilayer structure design based on a general machine-learning-kernel-based algorithm framework that can achieve the strong violation of Kirchhoff's radiation law in multiple bands with B =5T in a wide range of incident angles. The realization of multi-band and wide-angle nonreciprocal thermal radiation mainly depends on the magneto-optical effect and the excitation of cavity modes with different orders. In addition, through the study of the external magnetic field B, it is found that when B =3T, the structure can also achieve multi-band nonreciprocal thermal radiation. Moreover, single, double, and multiband nonreciprocal thermal radiation can be easily achieved using our proposed method by adjusting the number of layers, magnetic field strength, and material thickness. Our present optimization method can also be extended to the optimization of multilayer structures containing Weyl semimetals and may promote the development of multi-band and broadband nonreciprocal thermal emitters.

Declaration of Competing Interest

The authors declare that they have no known competing financial interests or personal relationships that could have appeared to influence the work reported in this paper.

CRediT authorship contribution statement

Zihe Chen: Conceptualization, Investigation, Methodology, Formal analysis, Writing – original draft, Writing – review & editing. **Shilv Yu:** Investigation, Writing – review & editing. **Bin Hu:** Writing – review & editing. **Run Hu:** Conceptualization, Project administration, Funding acquisition, Writing – review & editing.

Acknowledgments

The authors would like to acknowledge the financial support by National Natural Science Foundation of China (52211540005, 52076087), and the Open Project Program of Wuhan National Laboratory for Optoelectronics (2021WNLOKF004), Wuhan Knowledge Innovation Shuguang Program, and Science and Technology Program of Hubei Province (2021BLB176).

References

[1] G.I. Kirchhoff, On the relation between the radiating and absorbing powers of different bodies for light and heat, London, Edinburgh, Dublin Philos. Mag. J. Sci. 20 (1860) 1–21.
[2] Z.M. Zhang, X. Wu, C. Fu, Validity of Kirchhoff's law for semitransparent films made of anisotropic materials, J. Quant. Spectrosc. Radiat. Transfer 245 (2020) 106904.
[3] Z.M. Zhang, Nano/microscale Heat Transfer, Springer, Cham, 2020.
[4] S.E. Han, Theory of thermal emission from periodic structures, Phys. Rev. B 80 (15) (2009) 155108.
[5] Y. Park, B. Zhao, S. Fan, Reaching the Ultimate Efficiency of Solar Energy Harvesting with a Nonreciprocal Multijunction Solar Cell, Nano Lett 22 (1) (2022) 448–452.
[6] S. Jafari Ghalekohneh, B. Zhao, Nonreciprocal Solar Thermophotovoltaics, Phys. Rev. Appl. 18 (3) (2022) 034083.
[7] L. Zhu, S. Fan, Near-complete violation of detailed balance in thermal radiation, Phys. Rev. B 90 (22) (2014) 220301.
[8] J. Wu, F. Wu, T. Zhao, X. Wu, Tunable nonreciprocal thermal emitter based on metal grating and graphene, Int. J. Therm. Sci. 172 (2022) 107316.
[9] J. Wu, F. Wu, X. Wu, Strong dual-band nonreciprocal radiation based on a four-part periodic metal grating, Opt. Mater. 120 (2021) 111476.
[10] W. Han, L. Yazhou, H. Jianfei, Enhanced nonreciprocal thermal radiation properties of Graphene-based Magneto-optical materials, Opt. Laser Technol. 142 (2021) 107279.
[11] B. Zhao, C. Guo, C.A.C. Garcia, P. Narang, S. Fan, Axion-field-enabled nonreciprocal thermal radiation in Weyl semimetals, Nano Lett 20 (3) (2020) 1923–1927.
[12] M. Luo, Y. Xu, Y. Xiao, G. Yu, Strong nonreciprocal thermal radiation by optical Tamm states in Weyl semimetallic photonic multilayers, Int. J. Therm. Sci. 183 (2023) 107851.
[13] Y. Tsurimaki, X. Qian, S. Pajovic, F. Han, M. Li, G. Chen, Large nonreciprocal absorption and emission of radiation in type-I Weyl semimetals with time reversal symmetry breaking, Phys. Rev. B 101 (16) (2020) 165426.
[14] J. Wu, B. Wu, Z. Wang, X. Wu, Strong nonreciprocal thermal radiation in Weyl semimetal-dielectric multilayer structure, Int. J. Therm. Sci. 181 (2022) 107788.
[15] X. Wu, R. Liu, H. Yu, B. Wu, Strong nonreciprocal radiation in magnetophotonic crystals, J. Quant. Spectrosc. Radiat. Transfer 272 (2021) 107794.
[16] Q. Wang, Y. Xu, R. Lou, Z. Liu, M. Li, Y. Huang, D. Shen, H. Weng, S. Wang, H. Lei, Large intrinsic anomalous Hall effect in half-metallic ferromagnet $Co_3Sn_2S_2$ with magnetic Weyl fermions, Nat. Commun. 9 (1) (2018) 3681.
[17] R. Singha, S. Roy, A. Pariari, B. Satpati, P. Mandal, Magnetotransport properties and giant anomalous Hall angle in the half-Heusler compound TbPtBi, Phys. Rev. B 99 (3) (2019) 035110.
[18] A.K. Nayak, J.E. Fischer, Y. Sun, B. Yan, J. Karel, A.C. Komarek, C. Shekhar, N. Kumar, W. Schnelle, J. Kuebler, C. Felser, S.S.P. Parkin, Large anomalous Hall effect driven by a nonvanishing Berry curvature in the noncolinear antiferromagnet Mn_3Ge, Sci. Adv. 2 (4) (2016) e1501870.
[19] Y.-J. Liu, X. Xie, L. Xie, Z.-K. Yang, H.-W. Yang, Dual-band absorption characteristics of one-dimensional photonic crystal with graphene-based defect, Optik (Stuttg) 127 (9) (2016) 3945–3948.
[20] R. Ning, Z. Jiao, J. Bao, Tunable multi-band absorption in metasurface of graphene ribbons based on composite structure, Eur. Phys. J. Appl. Phys. 79 (1) (2017) 10201.
[21] Z.N. Zhang, L.X. Zhu, Broadband nonreciprocal thermal emission, Phys. Rev. Appl. 19 (1) (2023) 014013.
[22] J. Wu, Y.M. Qing, Strong nonreciprocal radiation with topological photonic crystal heterostructure, Appl. Phys. Lett. 121 (11) (2022) 112201.
[23] J. Wu, F. Wu, T. Zhao, M. Antezza, X. Wu, Dual-band nonreciprocal thermal radiation by coupling optical Tamm states in magnetophotonic multilayers, Int. J. Therm. Sci. 175 (2022) 107457.
[24] J. Wu, Z. Wang, B. Wu, Z. Shi, X. Wu, The giant enhancement of nonreciprocal radiation in Thue-morse aperiodic structures, Opt. Laser Technol. 152 (2022) 108138.
[25] B. Zhao, Y. Shi, J. Wang, Z. Zhao, N. Zhao, S. Fan, Near-complete violation of Kirchhoff's law of thermal radiation with a 0.3 T magnetic field, Opt. Lett. 44 (17) (2019) 4203–4206.
[26] M.Q. Liu, C.Y. Zhao, Near-infrared nonreciprocal thermal emitters induced by asymmetric embedded eigenstates, Int. J. Heat Mass Transfer 186 (2022) 122435.

[27] R. Hu, J.L. Song, Y.D. Liu, W. Xi, Y.T. Zhao, X.J. Yu, Q. Cheng, G.M. Tao, X.B. Luo, Machine learning-optimized Tamm emitter for high-performance thermophotovoltaic system with detailed balance analysis, Nano Energy 72 (2020) 104687.
[28] T.M. Dieb, S. Ju, J. Shiomi, K. Tsuda, Monte Carlo tree search for materials design and discovery, MRS Commun. 9 (2) (2019) 532–536.
[29] M. Yamawaki, M. Ohnishi, S. Ju, J. Shiomi, Multifunctional structural design of graphene thermoelectrics by Bayesian optimization, Sci. Adv. 4 (6) (2018) eaar4192.
[30] S. Ju, T. Shiga, L. Feng, Z. Hou, K. Tsuda, J. Shiomi, Designing nanostructures for phonon transport via bayesian optimization, Phys. Rev. X 7 (2) (2017) 021024.
[31] K. Leosson, S. Shayestehaminzadeh, T.K. Tryggvason, A. Kossoy, B. Agnarsson, F. Magnus, S. Olafsson, J.T. Gudmundsson, E.B. Magnusson, I.A. Shelykh, Comparing resonant photon tunneling via cavity modes and Tamm plasmon polariton modes in metal-coated Bragg mirrors, Opt. Lett. 37 (19) (2012) 4026–4028.